PHYSICAL REVIEW D **92,** 054001 (2015)

Revised model of absorption corrections for the $pp \to pp\pi^+\pi^-$ process

Piotr Lebiedowicz[*] and Antoni Szczurek[†]

Institute of Nuclear Physics PAN, PL-31-342 Kraków, Poland

(Received 11 May 2015; published 2 September 2015)

We include new additional absorption corrections into the double Pomeron/Reggeon exchange (nonresonant) model for $pp \to pp\pi^+\pi^-$ or $p\bar{p} \to p\bar{p}\pi^+\pi^-$ processes. They are related to the πN nonperturbative interaction in the final state of the reaction. We present predictions of cross sections for RHIC, Tevatron, and LHC experiments. The new absorption corrections lead to a further decrease of the cross section by about a factor of 2. The role of the absorption corrections is quantified for several differential distributions. They change the shape of some distributions ($d\sigma/dt$, $d\sigma/dp_{t,p}$, $d\sigma/d\phi_{pp}$) but leave almost unchanged shape of other distributions ($d\sigma/dM_{\pi\pi}$, $d\sigma/dy_{\pi}$, $d\sigma/dp_{t,\pi}$, $d\sigma/d\phi_{\pi\pi}$). The effect may have an important impact on the interpretation of the recent STAR and CDF data as well as the forthcoming data of the ALICE, ATLAS/ALFA, and CMS/TOTEM collaborations.

DOI: 10.1103/PhysRevD.92.054001 PACS numbers: 12.40.Nn, 13.60.Le, 14.40.Be

I. INTRODUCTION

There is a growing experimental and theoretical interest in an understanding of soft hadronic processes at high energy; for reviews, see, e.g., [1,2], and the references therein. One of the reactions which can be relatively easy to measure is $pp \to p\pi^+\pi^- p$ or $p\bar{p} \to p\pi^+\pi^-\bar{p}$ (four charged particles in the final state). There are several recently begun experimental projects by the COMPASS [3,4], STAR [5], CDF [6,7], ALICE [8,9], ATLAS [10], and CMS [11] collaborations which will measure differential cross sections for the reaction(s). Here, we wish to compare predictions of the double Pomeron/Reggeon exchange model[1] with the recent STAR and CDF data.

The principal reason for studying the central exclusive production of mesons is to search for glueballs [12]. There is some evidence, from an analysis of the decay modes of the scalar states observed, that the lightest scalar glueball manifests itself through the mixing with nearby $q\bar{q}$ states [13,14]. The exclusive production of lower mass scalar and pseudoscalar resonances within a tensor Pomeron approach [15] was recently examined in [16]. Resonant ($\rho^0 \to \pi^+\pi^-$) and nonresonant (Drell-Söding) photon-Pomeron/Reggeon production was studied in [17]. In Refs. [18,19] the continuum background to the production of the $\chi_c(0^+)$ state via two-body $\pi^+\pi^-$ and K^+K^- decays was considered. For exclusive production of other mesons, see, e.g., [20–22], where mainly the noncentral processes were discussed.

Some time ago we proposed a simple phenomenological model for the $\pi^+\pi^-$-continuum mechanism [see the diagrams in Fig. 1(a)] using the tools of Regge theory [23], where perturbative QCD cannot be reliably applied. For early studies of two-pion production, see Refs. [24–26]. In the Lebiedowicz-Szczurek model [23], the parameters of Pomeron and subleading Reggeon exchanges were adjusted to describe total and elastic πN scattering. The nonresonant model can be supplemented to include the pp or $p\bar{p}$ absorption effects [18,27]; see the diagrams in Fig. 1(b). The largest uncertainties in the model are due to the unknown off-shell pion form factor and the absorption corrections (the soft survival factor due to screening corrections). Usually, the absorption is done in the eikonal approximation. The absorption effects lead to substantial damping of the cross section. The damping depends on the collision energy and the kinematical variables. The model discussed here, with reasonable vertex form factors accounting for off-shellness of nonpointlike pions in the middle of the diagrams in Fig. 1, gives a rough description of the ISR data [28–30]. To get a reasonable description of currently existing experimental data, the parameter(s) of the form factors has (have) to be adjusted [18,27].

Recently, the Lebiedowicz-Szczurek model [23] was implemented in GenEx MC [31]. There, absorptive corrections are not taken into account explicitly. The authors of [32] constructed a DIME Monte Carlo code, where almost the same approach was implemented. In [32] a two-channel eikonal model was considered.

It is not clear if the absorption effects considered so far are sufficient for describing the data. Any interaction between participating particles potentially leads to absorptive effects, as it destroys the exclusivity of the process. In the present paper, we will include the additional absorption effects due to the strong nonperturbative interaction of charged pions and (anti-)protons in the final state (see the corresponding diagrams in Fig. 2), and we will quantify their role for an integrated cross section and for many

[*]Piotr.Lebiedowicz@ifj.edu.pl

[†]Also at University of Rzeszów, PL-35-959 Rzeszów, Poland. Antoni.Szczurek@ifj.edu.pl

[1]We use the name "Lebiedowicz-Szczurek model" to denote the proposed details of our approach in our previous papers.

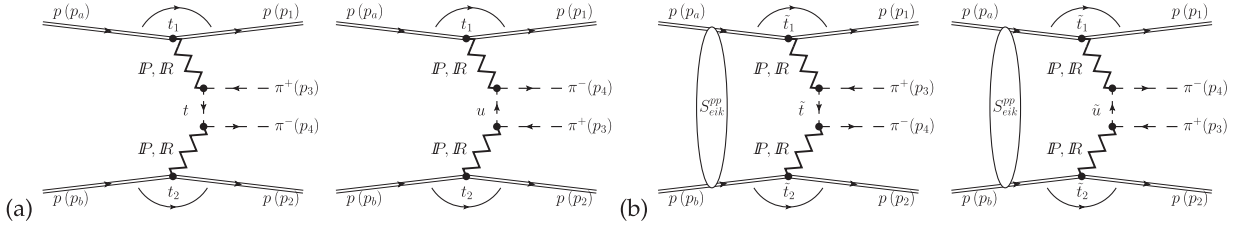

FIG. 1. (a) Born amplitudes for the $pp \to pp\pi^+\pi^-$ process. (b) Absorptive correction amplitudes due to the pp interaction.

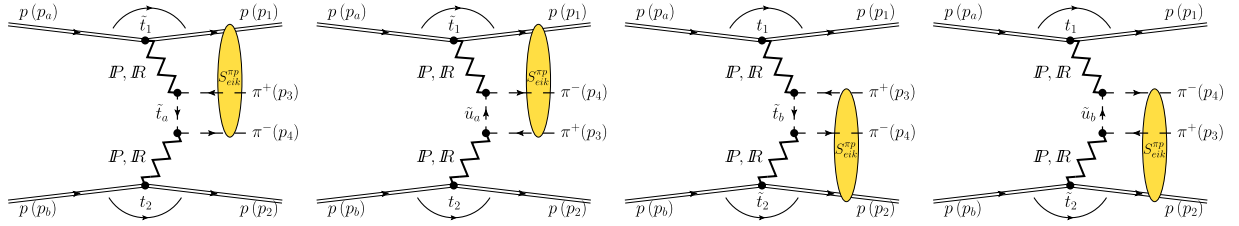

FIG. 2 (color online). New absorptive correction amplitudes for the $pp \to pp\pi^+\pi^-$ process due to the πp interaction in the final state included in the present analysis.

differential distributions for the considered process.[2] Our theoretical results will be compared to recent experimental results obtained by the STAR [5] and CDF [6,7] collaborations. We will also make some predictions for the ALICE, ATLAS, and CMS experiments.

II. BORN AMPLITUDE

The amplitude squared for the $pp \to pp\pi^+\pi^-$ process (with four-momenta $p_a + p_b \to p_1 + p_2 + p_3 + p_4$) considered within the framework of Regge theory with the central $\pi^+\pi^-$ system produced by the exchange of two Pomeron/Reggeons in the t channel, as shown in Fig. 1, can be written as

$$|\mathcal{M}|^2 = |\mathcal{M}_{I=0}|^2 + |\mathcal{M}_{I=1}|^2 + |\mathcal{M}_{I=2}|^2, \quad (2.1)$$

where the isospin amplitudes can be decomposed to the Regge ingredients as

$$\mathcal{M}_{I=0} = \mathcal{M}^{\mathbb{P}\mathbb{P}} + \mathcal{M}^{\mathbb{P}f_{2\mathbb{R}}} + \mathcal{M}^{f_{2\mathbb{R}}\mathbb{P}} + \mathcal{M}^{f_{2\mathbb{R}}f_{2\mathbb{R}}} + \langle 1,0;1,0|0,0\rangle \mathcal{M}^{\rho_{\mathbb{R}}\rho_{\mathbb{R}}}, \quad (2.2)$$

$$\mathcal{M}_{I=1} = \mathcal{M}^{\mathbb{P}\rho_{\mathbb{R}}} + \mathcal{M}^{\rho_{\mathbb{R}}\mathbb{P}} + \mathcal{M}^{f_{2\mathbb{R}}\rho_{\mathbb{R}}} + \mathcal{M}^{\rho_{\mathbb{R}}f_{2\mathbb{R}}}, \quad (2.3)$$

$$\mathcal{M}_{I=2} = \langle 1,0;1,0|2,0\rangle \mathcal{M}^{\rho_{\mathbb{R}}\rho_{\mathbb{R}}}. \quad (2.4)$$

The Clebsch-Gordan coefficients $\langle I_1, I_{31}; I_2, I_{32}|I, I_3\rangle$ are $\langle 1,0;1,0|0,0\rangle = -\sqrt{1/3}$ and $\langle 1,0;1,0|2,0\rangle = \sqrt{2/3}$. The situation can be summarized as

$$|\mathcal{M}_{I=0}|^2 \gg |\mathcal{M}_{I=1}|^2 \gg |\mathcal{M}_{I=2}|^2. \quad (2.5)$$

For the dominant Pomeron-Pomeron contribution we have C parity $C = +1$ and isospin $I = 0$ of the produced $\pi^+\pi^-$ system. In general, not only do the leading double Pomeron exchanges contribute, but the subleading $f_{2\mathbb{R}}$ ($C = +1$) and $\rho_{\mathbb{R}}$ ($C = -1$) Reggeon exchanges do as well.[3]

The Born amplitude with the intermediate pion exchange can be written as

[2]We recall that the absorptive corrections caused by the pion-proton interactions were discussed previously in Sec. 5.2 of [19], where the "enhanced" screening corrections caused by the exchange between the upper (lower) proton and the lower (upper) Pomeron were also mentioned. The authors of [19] expected the size of both screening effects to be suppressed in the kinematic domains considered in [19]; therefore, they did not account for such effects. In our paper we will estimate the absorptive corrections due to the proton-pion rescattering and will discuss their influence on distributions in different kinematic variables; see Sec. IV.

[3]The $\rho_{\mathbb{R}}\rho_{\mathbb{R}}$ component is negligible (see the strength parameters in Table 2.1 of [27]) and was omitted in our analysis. We emphasize that at lower energies (COMPASS, ISR) the subleading $f_{2\mathbb{R}}$ exchanges constitute a large contribution to the total cross section and must be included in addition to the Pomeron exchanges; see, e.g., Sec. 2.3 of [27]. Furthermore, there is a large interference effect between the different components in the amplitude of about 50% (the total cross section in full phase space); see Sec. 2.6.2 of [27]. As we shall see in the results section, imposing limitations on pion rapidity $|y_\pi| < 1$ and going to higher energies reduces the role of subleading $f_{2\mathbb{R}}$ exchanges; however, because of their non-negligible interference effects with the leading $\mathbb{P}\mathbb{P}$ term, we keep them explicitly in our calculations.

$$\mathcal{M}^{\rm Born}_{pp\to pp\pi^+\pi^-} = M_{13}(s_{13},t_1)\frac{F_\pi^2(t)}{t-m_\pi^2}M_{24}(s_{24},t_2) + M_{14}(s_{14},t_1)\frac{F_\pi^2(u)}{u-m_\pi^2}M_{23}(s_{23},t_2), \quad (2.6)$$

where the subsystem amplitudes $M_{ij}(s_{ij},t_i)$ denotes "interaction" between the forward proton ($i=1$) or the backward proton ($i=2$) and one of the two pions ($j=3$ for π^+ or $j=4$ for π^-). Not all combinations of the interactions are shown in Fig. 1(a). Some absorptive effects are included inherently in our calculation by using an effective interaction fitted to describe the πN elastic scattering data. The model assumes that the interaction of the proton with the nearest pion, like p_1 with p_3, is already accounted for in the parametrization of the "elementary" proton-pion amplitude. The energy dependence of the πp subsystem amplitudes M_{ij} is parametrized in terms of the Pomeron and the $f_{2\mathbb{R}}$ Reggeon exchange

$$M_{ij}(s_{ij},t_i) = \eta_{\mathbb{P}} s_{ij} C^{\pi N}_{\mathbb{P}}\left(\frac{s_{ij}}{s_0}\right)^{\alpha_{\mathbb{P}}(t_i)-1}\exp\left(\frac{B^{\pi N}_{\mathbb{P}}}{2}t_i\right) + \eta_{f_{2\mathbb{R}}} s_{ij} C^{\pi N}_{f_{2\mathbb{R}}}\left(\frac{s_{ij}}{s_0}\right)^{\alpha_{f_{2\mathbb{R}}}(t_i)-1}\exp\left(\frac{B^{\pi N}_{f_{2\mathbb{R}}}}{2}t_i\right), \quad (2.7)$$

where $\eta_{\mathbb{P}} = i, \eta_{f_{2\mathbb{R}}} = i - \cot\left[\frac{\pi}{2}\alpha_{f_{2\mathbb{R}}}(0)\right]$,[4] s_{ij} is the energy in the (ij) subsystem, and the energy scale s_0 is fixed at $s_0 = 1\ \mathrm{GeV}^2$. The Pomeron and Reggeon trajectories, $\alpha_{\mathbb{P}}(t)$ and $\alpha_{f_{2\mathbb{R}}}(t)$, respectively, are assumed to be of a standard linear form; see, for instance [33],

$$\alpha_{\mathbb{P}}(t) = \alpha_{\mathbb{P}}(0) + \alpha'_{\mathbb{P}}t, \qquad \alpha_{\mathbb{P}}(0) = 1.0808, \quad \alpha'_{\mathbb{P}} = 0.25\ \mathrm{GeV}^{-2}, \quad (2.8)$$

$$\alpha_{f_{2\mathbb{R}}}(t) = \alpha_{f_{2\mathbb{R}}}(0) + \alpha'_{f_{2\mathbb{R}}}t, \qquad \alpha_{f_{2\mathbb{R}}}(0) = 0.5475, \quad \alpha'_{f_{2\mathbb{R}}} = 0.93\ \mathrm{GeV}^{-2}. \quad (2.9)$$

We found the slope parameters $B^{\pi N}_{\mathbb{P}/f_{2\mathbb{R}}}$ from a fitting of the elastic $\pi^\pm p$ differential cross sections:

$$B^{\pi N}_{\mathbb{P}} = 5.5\ \mathrm{GeV}^{-2}, \qquad B^{\pi N}_{f_{2\mathbb{R}}} = 4\ \mathrm{GeV}^{-2}. \quad (2.10)$$

Our model makes various simplifications, but it describes the data for elastic πN scattering fairly well for energies $\sqrt{s_{\pi N}} \gtrsim 2.5$ GeV (see Fig. 2.2 of [27]).

So far, we have assumed a simple exponential dependence of the πN subprocess amplitudes (2.7) which is valid only for small $|t|$ ($0.01 < -t < 0.4\ \mathrm{GeV}^2$). At larger $|t|$ (t_1 or t_2 in the $2\to4$ case), the mechanism becomes more complicated. Here, a subsequent exchange of two Pomerons and the exchange of the Pomeron together with the Reggeon, or even pQCD effects (two-gluon exchange), may show up.[5] To have a more realistic t dependence, we suggest the following replacement in the leading Pomeron term (see also [44]):

$$\exp\left(\frac{B^{\pi N}_{\mathbb{P}}}{2}t_i\right)\left(\frac{s_{ij}}{s_0}\right)^{\alpha'_{\mathbb{P}}t_i} \to f(t_i,s_{ij}) = \exp\left(\mu^2 B(s_{ij})\right)\exp\left(-\mu^2 B(s_{ij})\sqrt{1-\frac{t_i}{\mu^2}}\right); \quad B(s_{ij}) = B_0 + 2\alpha'_{\mathbb{P}}\ln\left(\frac{s_{ij}}{s_0}\right), \quad (2.11)$$

where the free parameters μ, B_0 have been adjusted to the πN elastic scattering data, as illustrated in Fig. 3. In the calculations of the elastic $\pi^\pm p$ cross sections, the Pomeron, $f_{2\mathbb{R}}$, and $\rho_{\mathbb{R}}$ Reggeon exchanges were included. The so-called stretched exponential parametrization $f(t_i,s_{ij})$ coincides at low $|t|$ with the simple exponential form, while at larger $|t|$ a harder tail appears. This function is close to a parametrization $\sim\exp(-bp_t)$ suggested by Orear [45] for elastic pp scattering at large $|t|$. The πp data show a diffractive dip at $-t\sim4\ \mathrm{GeV}^2$.

The extra form factors $F_\pi(t)$ and $F_\pi(u)$ in Eq. (2.6) "correct" for the off-shellness of the intermediate pions. The form of the form factors is unknown, particularly at higher values of t or u, and the form factors are parametrized here in two ways:

$$F_\pi(t) = \exp\left(\frac{t-m_\pi^2}{\Lambda^2_{\mathrm{off},E}}\right), \quad (2.12)$$

$$F_\pi(t) = \frac{\Lambda^2_{\mathrm{off},M}-m_\pi^2}{\Lambda^2_{\mathrm{off},M}-t}, \quad (2.13)$$

and for $F_\pi(u)$ we have to replace $t\longleftrightarrow u$. These form factors are normalized to unity on the pion-mass shell $F_\pi(m_\pi^2)=1$. In general, the parameter Λ_{off} is not known precisely but, in principle, could be fitted to the normalized experimental data. How to extract the off-shell parameters will be discussed in the results section.

[4] In general, $\eta_{\mathbb{P}}$ and $\eta_{f_{2\mathbb{R}}}$ depend on t_i. At present, we use the simplified version of the πN interaction. This version was used to fit elastic πN scattering experimental data (see Fig. 3).

[5] Description of the elastic pp and $p\bar{p}$ scattering data is rather difficult. In Ref. [39] the authors presented a model including $\mathbb{P}+\mathbb{P}\mathbb{P}+ggg$ terms and the linear Pomeron trajectory. Alternative approaches [40,41] combine the soft and hard Pomeron exchanges or the odderon exchange in addition [42]. In the latter case, the authors also considered various forms of the nonlinear Pomeron trajectory. In [43] the role of the eikonalization of the pp amplitude in both one- and two-channel eikonal models were discussed.

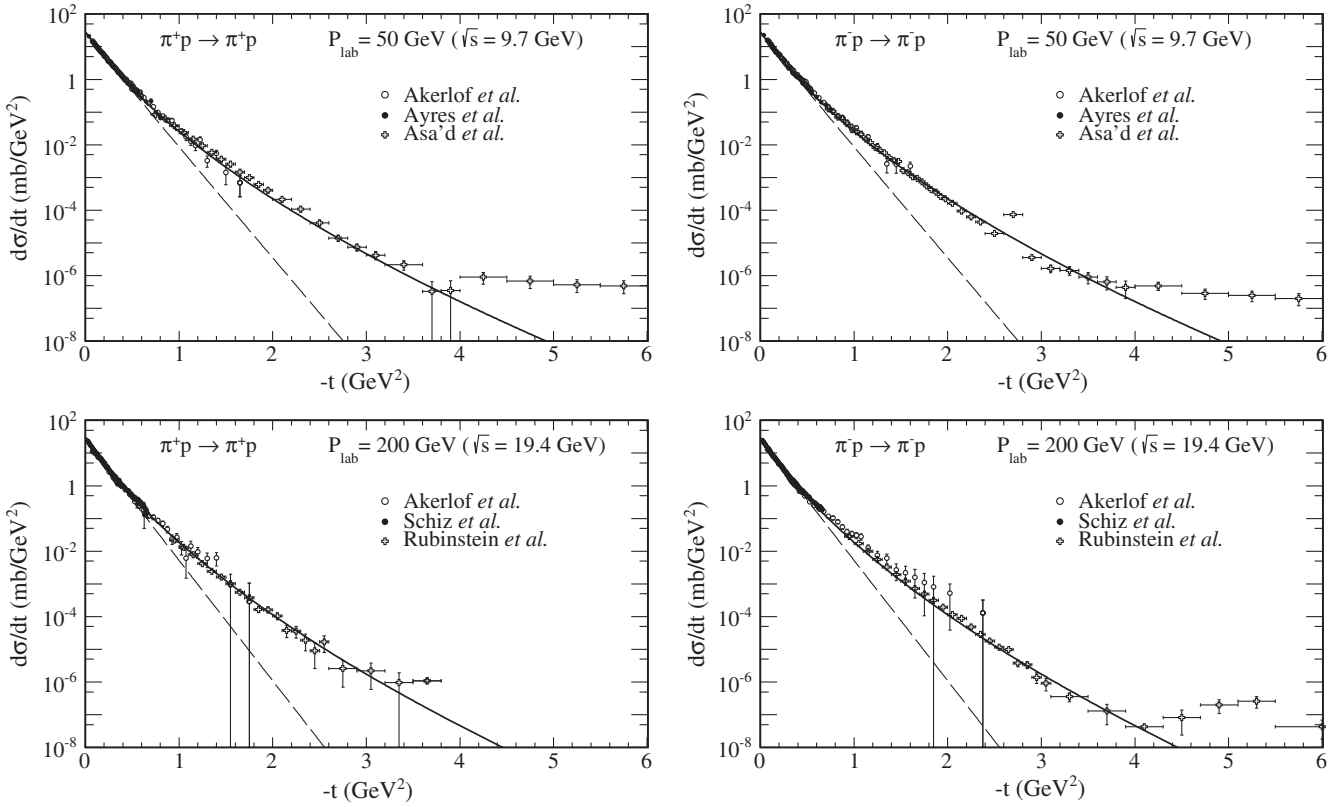

FIG. 3. Differential distributions $d\sigma/dt$ for $\pi^+ p$ (left panel) and $\pi^- p$ (right panel) elastic scattering at incident beam momenta $P_{\rm lab} = 50$ GeV ($\sqrt{s} \simeq 9.7$ GeV) [34–36] and $P_{\rm lab} = 200$ GeV ($\sqrt{s} \simeq 19.4$ GeV) [34,37,38]. The dashed lines show results obtained with formula (2.10), while the solid lines are obtained via the replacement (2.11), where $B_0 = 6.5$ GeV^{-2} and $\mu^2 = 0.6$ GeV^2.

In our calculations, for simplicity, we have used the normal pion propagator [see Eq. (2.6)] without the Reggeization of the intermediate off-shell pions in the t channel. In general, other meson exchanges should be included in the model, e.g., a $\mathbb{P}$-a_2-$\mathbb{P}$ exchange, as was discussed in [46]. The details of how to include the Reggeization of the (virtual) meson exchanges are given in, e.g., [46]. There is also other element which can be potentially added to the model: the possibility of producing additional particles in the double Pomeron/Reggeon into the $\pi^+\pi^-$ subprocesses. To account for the fact that only two pions (without any additional secondaries) are produced in the central double Pomeron/Reggeon fusion, we have introduced in our calculations, following [19], an extra suppression factor in the exponential form: $f(M_{\pi\pi}) = \exp(-c \ln(M_{\pi\pi}/M_0))$, $M_0 = 0.8$ GeV^2. The parameter c defines the strength of the suppression and can, in principle, be extracted from experimental data. In the present calculations, we take $c = 0.5$. We wish to emphasize that the suppression factor $f(M_{\pi\pi})$ is included only in separate curves that demonstrated its role and not included in other cases.

III. ABSORPTION CORRECTIONS

The absorption amplitude including the πN interactions can be written in a similar way as that in the case of pp ($p\bar{p}$) interaction, i.e., in the eikonal form

$$\begin{aligned}\mathcal{M}^{\pi p\text{-rescattering}}_{pp\to pp\pi^+\pi^-} \approx{}& \frac{i}{16\pi^2 s_{14}} \int d^2k_t \mathcal{M}^{\rm Born}_{pp\to pp\pi^+\pi^-}(s,\tilde{t}_1,t_2,\tilde{t}_a)\mathcal{M}^{\mathbb{P}\text{-exchange}}_{\pi^- p\to\pi^- p}(s_{14},k_t^2) \\ &+ \frac{i}{16\pi^2 s_{13}} \int d^2k_t \mathcal{M}^{\rm Born}_{pp\to pp\pi^+\pi^-}(s,\tilde{t}_1,t_2,\tilde{u}_a)\mathcal{M}^{\mathbb{P}\text{-exchange}}_{\pi^+ p\to\pi^+ p}(s_{13},k_t^2) \\ &+ \frac{i}{16\pi^2 s_{23}} \int d^2k_t \mathcal{M}^{\rm Born}_{pp\to pp\pi^+\pi^-}(s,t_1,\tilde{t}_2,\tilde{t}_b)\mathcal{M}^{\mathbb{P}\text{-exchange}}_{\pi^+ p\to\pi^+ p}(s_{23},k_t^2) \\ &+ \frac{i}{16\pi^2 s_{24}} \int d^2k_t \mathcal{M}^{\rm Born}_{pp\to pp\pi^+\pi^-}(s,t_1,\tilde{t}_2,\tilde{u}_b)\mathcal{M}^{\mathbb{P}\text{-exchange}}_{\pi^- p\to\pi^- p}(s_{24},k_t^2). \end{aligned} \tag{3.1}$$

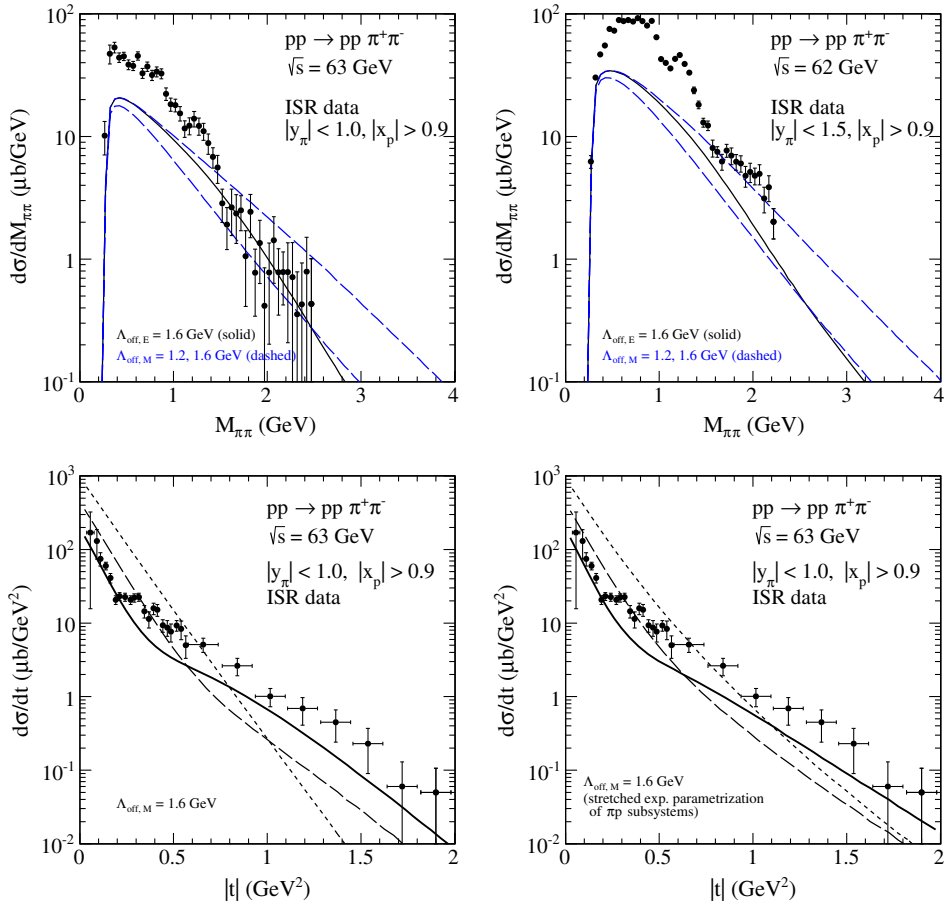

FIG. 4 (color online). Two-pion invariant mass distribution at ISR energies with the ISR kinematical cuts indicated in the legend. The ISR data [28,30] are shown for comparison. The blue dashed lines represent the results obtained for the monopole form factors [(2.13), $\Lambda_{\mathrm{off},M} = 1.2$ and 1.6 GeV], while the black solid lines are for the exponential form [(2.12), $\Lambda_{\mathrm{off},E} = 1.6$ GeV]. The bottom panels represent the $|t|$ distributions without (dotted lines) and with (dashed lines) the pp absorption corrections, and with all (pp and πN) absorption corrections included (solid lines). Results for the exponential (left panel) and for the stretched exponential (right panel) parametrizations of the πp subsystem are shown in addition.

In formula (3.1) we have indicated explicitly only crucial variables, mostly those arguments of $\mathcal{M}_{pp\to pp\pi^+\pi^-}$ which get modified in comparison to the Born amplitude (2.6). For example, the four-momenta squared of the Regge exchange in the first stage of the interaction (see Fig. 2) get modified as

$$\tilde{t}_1 = (\tilde{p}_1 - p_a)^2, \qquad \tilde{t}_2 = (\tilde{p}_2 - p_b)^2, \tag{3.2}$$

where the four-momenta of the intermediate nucleons are $\tilde{p}_1 = p_1 - k_t$ and $\tilde{p}_2 = p_2 - k_t$. Here, we have introduced the auxiliary four-vector $k_t = (0, \vec{k}_t, 0)$ to write formulas in a compact way. Similarly, the modified four-momenta of pions being propagated in the middle of the four-body $pp \to pp\pi^+\pi^-$ subprocess can be calculated as

$$\begin{aligned} \tilde{t}_a &= (\tilde{q}_1 - p_3)^2, \qquad \tilde{u}_a = (\tilde{q}_1 - p_4)^2, \\ \tilde{t}_b &= (\tilde{q}_2 - p_4)^2, \qquad \tilde{u}_b = (\tilde{q}_2 - p_3)^2, \end{aligned} \tag{3.3}$$

where $\tilde{q}_1 = p_a - \tilde{p}_1$ and $\tilde{q}_2 = p_b - \tilde{p}_2$ are the four-momenta of the (incoming) Regge exchanges. We leave all other not explicitly indicated variables which appear in the Born amplitude(s) unchanged. This is an approximation, but it is sufficient for the purpose of the present first exploratory analysis.

The full amplitude includes all rescattering corrections,

$$\begin{aligned} \mathcal{M}_{pp\to pp\pi^+\pi^-} = \mathcal{M}^{\mathrm{Born}}_{pp\to pp\pi^+\pi^-} &+ c_{pp}\mathcal{M}^{pp\text{-rescattering}}_{pp\to pp\pi^+\pi^-} \\ &+ c_{\pi p}\mathcal{M}^{\pi p\text{-rescattering}}_{pp\to pp\pi^+\pi^-}. \end{aligned} \tag{3.4}$$

In principle, the contributions due to the intermediate proton(s) diffractive excitation(s) ($p \to N^*$) could be effectively included by increasing the prefactors. In the present paper we shall take, however, $c_{pp} = c_{\pi p} = 1$.[6]

[6]How the extra multiplication of the absorption amplitude $\mathcal{M}^{pp\text{-rescattering}}_{pp\to pp\pi^+\pi^-}$ by a factor $c_{pp} = 1.2$ modifies the features of differential distributions was shown in [27]; see, e.g., Figs. 2.48, 2.49, and 2.50, and Table 2.5.

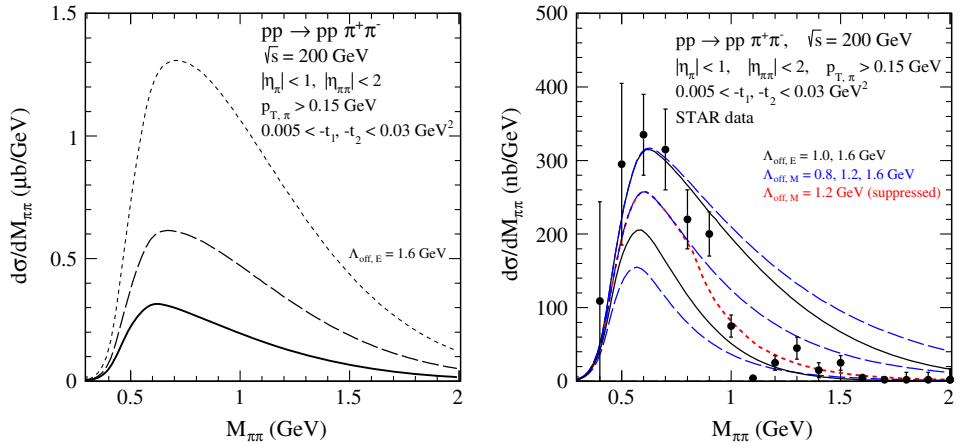

FIG. 5 (color online). Two-pion invariant mass distribution at $\sqrt{s} = 200$ GeV with the STAR kinematical cuts specified in the legend. The dotted line in the left panel corresponds to the Born calculation, the long-dashed and solid lines to calculations with the absorption effects due to the pp and the πp rescattering, respectively. In the right panel, the blue dashed lines represent the results with all absorption effects and obtained for the monopole form factors (2.13) for different choices of the cutoff parameter $\Lambda_{\mathrm{off},M} = 0.8, 1.2, 1.6$ GeV (from bottom to top). The red dotted line represents result for $\Lambda_{\mathrm{off},M} = 1.2$ GeV multiplied by the extra suppression factor $f(M_{\pi\pi})$, as explained in the text. The black solid lines are for the exponential form (2.12), and $\Lambda_{\mathrm{off},E} = 1.0$ and 1.6 GeV. The STAR preliminary data [5] are shown for comparison.

In the next section we shall show the effect of inclusion of the extra absorption terms on the total cross section, as well as on differential distributions. They lead to a further decrease of the cross section for the $pp \to pp\pi^+\pi^-$ or $p\bar{p} \to p\bar{p}\pi^+\pi^-$ reactions. We expect that the effects may be very important when comparing results of our calculation with the recent STAR and CDF experimental data, as well as with the forthcoming data of the ALICE, CMS, and ATLAS collaborations.

IV. PREDICTIONS FOR DIFFERENT EXPERIMENTS

In this section we shall present some selected results for the discussed exclusive processes calculated for kinematic domains relevant for the STAR, CDF, ALICE, CMS, and ATLAS experiments. In particular, we wish to concentrate on the effect of the new absorption corrections due to the pion–(anti-)proton interaction.

Before we go to the higher energies, let us first discuss old ISR data [28,30]. In Fig. 4 (the top panels), we show results for two-pion invariant mass distributions. The theoretical calculations including absorption corrections have been compared with the ISR data. In the calculations, two forms of the form factor for the off-shell pions were fixed as specified in the figure captions. The choice of form factor leads to different behavior at higher $M_{\pi\pi}$. We also show (in the bottom panels) the result for the exponential and "stretched exponential" t dependences without and with absorption corrections. The shape of the t distributions is strongly modified by the absorption corrections and is similar to that obtained in the ISR experiment.

A. STAR experiment

In Fig. 5 we present the invariant mass distributions of the pion pair produced in the $pp \to pp\pi^+\pi^-$ reaction for the STAR kinematics ($\sqrt{s} = 200$ GeV, $|\eta_\pi| < 1$ and $p_{t,\pi} > 0.15$ GeV for both pions, the pseudorapidity of the central $\pi^+\pi^-$ system $|\eta_{\pi\pi}| < 2$, and in the four-momentum transfer range $0.005 < -t_1, -t_2 < 0.03\,\mathrm{GeV}^2$). In the left panel, we show result obtained in the Born approximation (the dotted line), the result when including proton-proton interactions (the long-dashed line), and when including extra pion-nucleon interactions (the solid line) discussed in the present paper. We observe a significant damping of the cross section as well as a small shift of the maximum towards smaller invariant masses. In the right panel, we show results for different parameters of the off-shell form factors, together with the STAR preliminary data. One can observe that our predictions are quite sensitive to the form of the off-shell pion form factor (2.12) or (2.13) and depend on the value of the cutoff parameters Λ_{off}. If we describe the maximum of the cross section around $M_{\pi\pi} \sim 0.6$–0.7 GeV, we overestimate the cross section in the interval $1 < M_{\pi\pi} < 2$ GeV—essentially for both choices of the form factor form. A part of the effect may be related to an enhancement of the cross section due to $\pi\pi$ low-energy final state interaction.[7] This goes beyond the scope of the present paper, which concentrates on the new absorption effects.

[7]The low-energy $\pi\pi$ final state interaction was discussed in, e.g., [23,25,47].

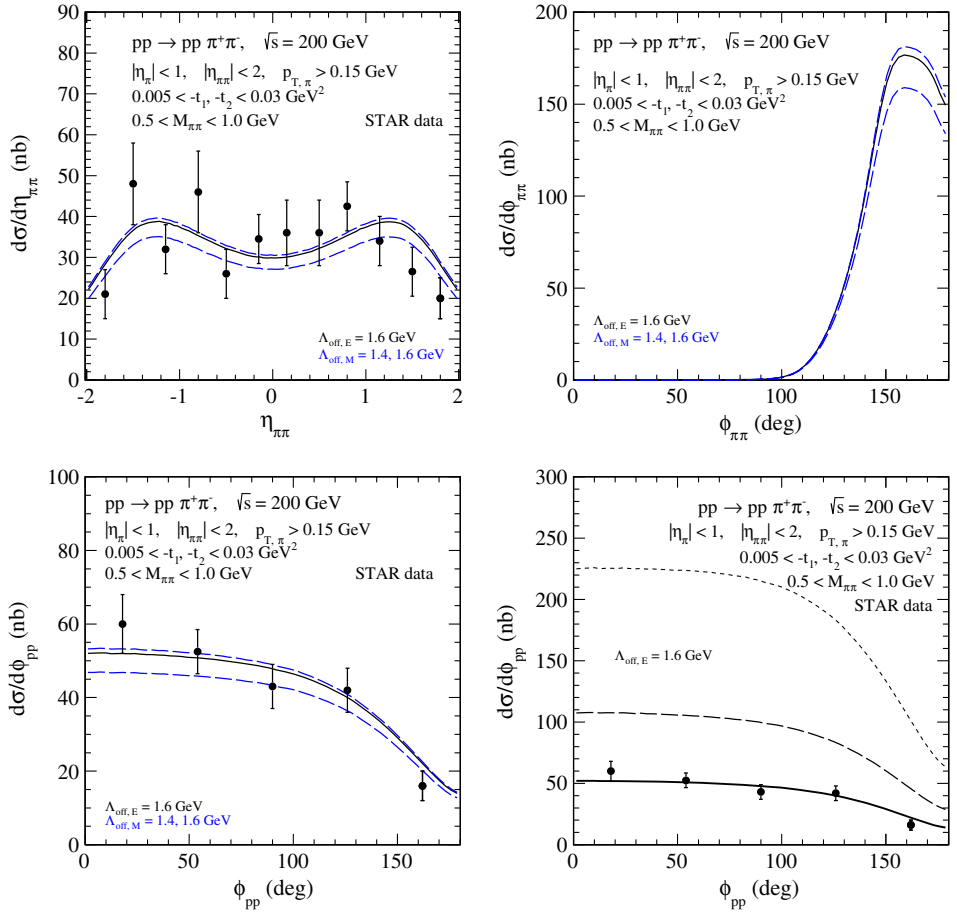

FIG. 6 (color online). The distributions in the pseudorapidity of the produced $\pi^+\pi^-$ system ($\eta_{\pi\pi}$) and in the azimuthal angle between the outgoing pions ($\phi_{\pi\pi}$) and between the outgoing protons (ϕ_{pp}) at $\sqrt{s} = 200$ GeV in the range of $0.5 < M_{\pi\pi} < 1$ GeV. In the right bottom panel, we show the results without the absorption effects (the dotted line), with the pp rescattering (the long-dashed line), and with the additional πp rescattering (the solid line). The STAR preliminary data [5] are shown for comparison.

In Fig. 6 (the left panel), we show the differential cross section for the exclusive production of the $\pi^+\pi^-$ system as a function of its pseudorapidity. We conclude that in the range $0.5 < M_{\pi\pi} < 1$ GeV, both forms of the off-shell pion form factor [(2.12) and (2.13)] describe the data well for $\Lambda_{\rm off} = 1.4$–1.6 GeV. However, the agreement seems a bit misleading in light of the disagreement in the invariant mass distribution discussed above. As will be discussed in this paper, the absorption effects usually strongly modify the distribution in the relative azimuthal angle between the outgoing protons ϕ_{pp} and leave the shape of the $\phi_{\pi\pi}$ distribution almost unchanged. For the STAR experiment (phase I), where there is a visible kinematical range—that is, at very small four-momentum transfers $|t|$—one can observe only a damping of the cross section (the right bottom panel). The decrease of $d\sigma/d\phi_{pp}$ and $d\sigma/d\phi_{\pi\pi}$ at $\phi \sim \pi$ is due to the STAR condition $|\eta_{\pi\pi}| < 2$. We have checked numerically that when $|\eta_{\pi\pi}|$ is large, then $\phi \sim \pi$. Cutting off large values of $|\eta_{\pi\pi}|$, therefore, as for the STAR experiment, damps the region of $\phi \sim \pi$, as observed in the lower panels of Fig. 6.

B. CDF experiment

We wish to emphasize that in this experiment, in contrast to the STAR experiment, the final state nucleons were not detected and only the rapidity gap conditions ($\Delta\eta > 4.6$ on each side of the $\pi^+\pi^-$) were imposed experimentally. In Fig. 7 (the left panel), we show the two-pion invariant mass distribution at $\sqrt{s} = 1.96$ TeV for the $p\bar{p} \to p\bar{p}\pi^+\pi^-$ reaction and with the following CDF cuts on kinematical variables: $p_{t,\pi} > 0.4$ GeV, $|\eta_\pi| < 1.3$ for both mesons, and $|y_{\pi\pi}| < 1$. The rapidity of the central $\pi^+\pi^-$ system is expressed by the formula

$$y_{\pi\pi} = \frac{1}{2}\ln\left(\frac{(p_{30} + p_{40}) + (p_{3z} + p_{4z})}{(p_{30} + p_{40}) - (p_{3z} + p_{4z})}\right), \qquad (4.1)$$

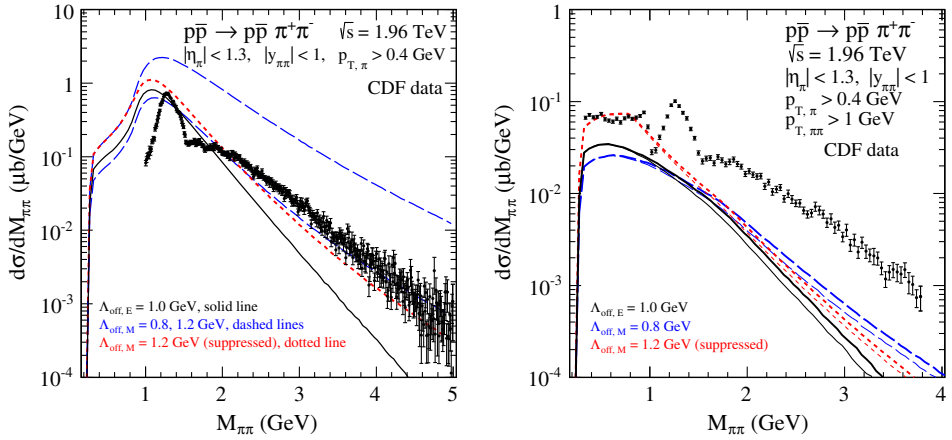

FIG. 7 (color online). Two-pion invariant mass distribution at $\sqrt{s} = 1.96$ TeV, with the CDF kinematical cuts specified in the legend. The meaning of the lines in the left panel is the same as in Fig. 5 (the right panel). In the right panel we show the results with an additional cut on transverse momentum of the pion pair $p_{t,\pi\pi} > 1$ GeV and for two different t dependences of the πp-subsystem amplitudes. The thick upper lines represent results for the replacement (2.11), while the thin lower lines show the results with formula (2.10). The CDF data [6,7] are shown with only statistical errors; systematic uncertainties are approximately 10% at all masses.

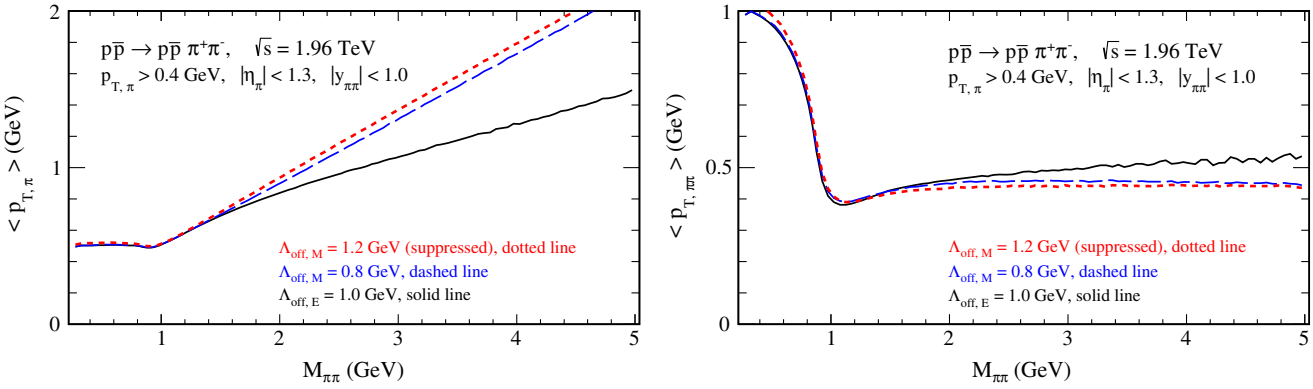

FIG. 8 (color online). Mean value of $p_{t,\pi}$ (left panel) and $p_{t,\pi\pi}$ (right panel) as a function of two-pion invariant mass at $\sqrt{s} = 1.96$ TeV calculated with the CDF kinematical cuts specified in the legend.

with the four-momenta p_3 (π^+ meson) and p_4 (π^- meson). The kinematical cuts $p_{t,\pi} > 0.4$ GeV on both pions strongly distort the region of low $M_{\pi\pi} < 1$ GeV. At $M_{\pi\pi} \simeq 1$ GeV, the data show a minimum due to interference of the $f_0(980)$ resonance contribution with the nonresonant background contribution. At higher $M_{\pi\pi}$, in the region of 1.2–1.7 GeV, some structures could be attributed to the $f_2(1270)$, $f_0(1370)$, $f_0(1500)$, and $f_0(1710)$ resonant states. The $f_0(1500)$ and $f_0(1710)$ mesons are considered to be scalar glueball candidates [13], but mixing with quarkonium states complicates the issue.

We roughly describe the differential cross section in the left panel when using the form factors (2.13) with $\Lambda_{\mathrm{off},M} \simeq 0.8$ GeV. The data at $\sqrt{s} = 0.9$ TeV look similar (see Fig. 1 of [7]). In the right panel of Fig. 7, we show results with an extra lower cut on the $\pi^+\pi^-$ transverse momentum. The results for the form factors that give a reasonable description in the left panel (without the cut) badly fail to describe the data in the right panel, underestimating the CDF data by a factor of about 5. In this case our model results are much below the experimental data, which could be due to a contamination of nonexclusive processes[8] and/or the perturbative mechanism discussed in [19,48]. Both the interference of the resonant state with the $\pi^+\pi^-$ continuum and the diffractive

[8]The experimental data at both energies may include, to some extent, diffractive dissociation of proton and antiproton (all of the produced unobserved hadrons have $|\eta| > 5.9$ [7]). In particular, they may contain processes leading to excitations of low diffractive masses of the baryonic systems, especially at $\sqrt{s} = 1.96$ TeV, where the experimental coverage of the phase space is lower. The experimental rapidity gap condition covers only a part of the available phase space.

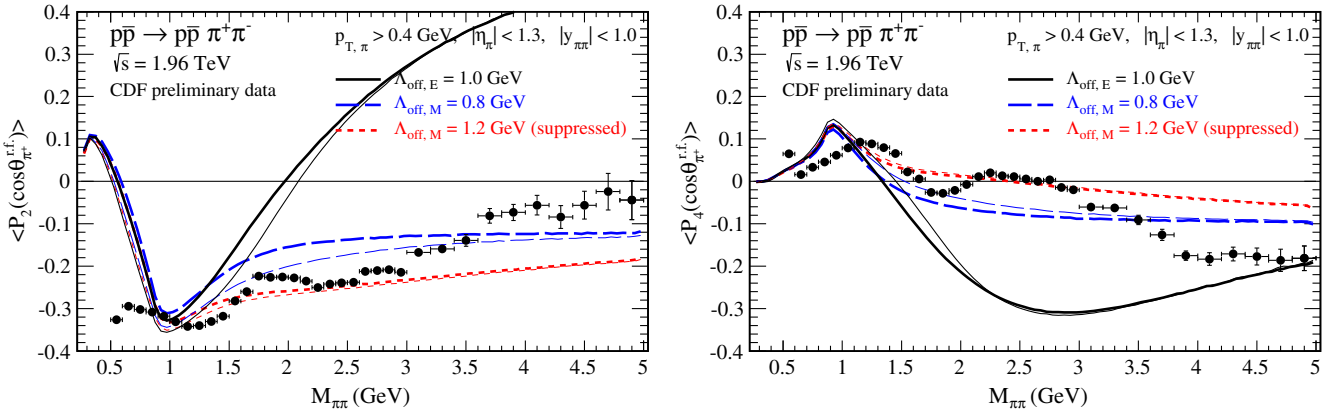

FIG. 9 (color online). Mean value of the first even Legendre polynomials $P_L(\cos\theta^{r.f.}_{\pi^+})$ as a function of the two-pion invariant mass, with the CDF kinematical cuts specified in the legend. The results correspond to two types of off-shell pion form factors: the exponential one (2.12) and the monopole one (2.13) without (thin lines) and with (thick lines) absorption effects. The red dotted line represents the result for the monopole type of form factor and with an extra suppression factor $f(M_{\pi\pi})$. The CDF preliminary data [6] are shown for comparison.

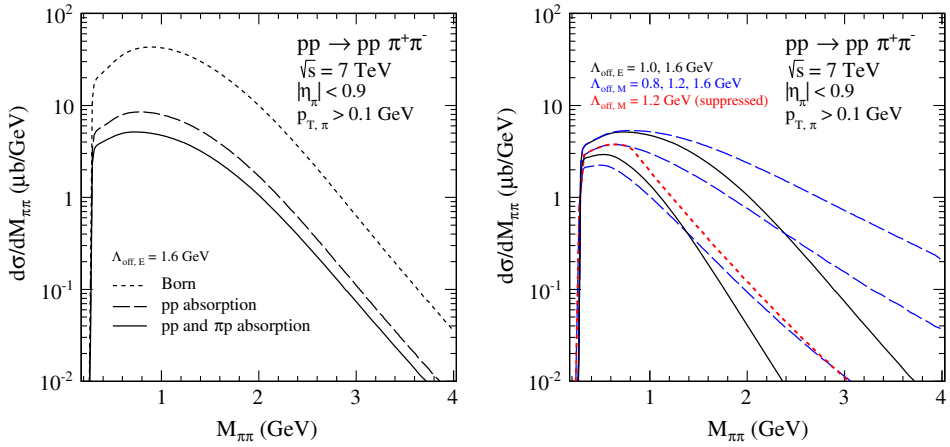

FIG. 10 (color online). Two-pion invariant mass distribution at $\sqrt{s} = 7$ TeV with the ALICE kinematical cuts specified in the legend. In the left panel we show results with a cutoff parameter $\Lambda_{\mathrm{off},E} = 1.6$ GeV [see (2.12)], without the absorption effects (the dotted line), with the pp rescattering (the long-dashed line), and with the additional πp rescattering (the solid line). The meaning of the lines in the right panel is the same as in Fig. 5.

dissociation effects require a more subtle theoretical approach. This will be addressed elsewhere. Thus, our nonresonant model should not be expected to fit the data precisely.

Now let us briefly discuss quantities or observables that are sensitive to the pion off-shell form factors. The dependence of $\langle p_{t,\pi}\rangle$ and $\langle p_{t,\pi\pi}\rangle$ as a function of the two-pion invariant mass is presented in Fig. 8. Our calculation shows a rise of the average pion transverse momentum with the dipion invariant mass. A dependence on the form of the form factor is clearly seen. On the contrary, the average transverse momentum of the dipion pair is almost independent of the form of the form factor and is a parameter of the form factor. This can be understood from the momentum conservation. The transverse momentum of the dipion system must be balanced by the transverse momenta of protons. The latter distributions (shapes) are obviously independent of the pion off-shell form factors.

Another observable which can be very sensitive to the choice of off-shell pion form factors are the Legendre polynomial $\langle P_{L_{\mathrm{even}}}(\cos\theta^{r.f.}_{\pi^+})\rangle(M_{\pi\pi})$ distributions, where $\cos\theta^{r.f.}_{\pi^+}$ is the angle of the π^+ meson with respect to the beam axis, in the $\pi^+\pi^-$ rest frame. In Fig. 9 we present the average P_L, calculated as

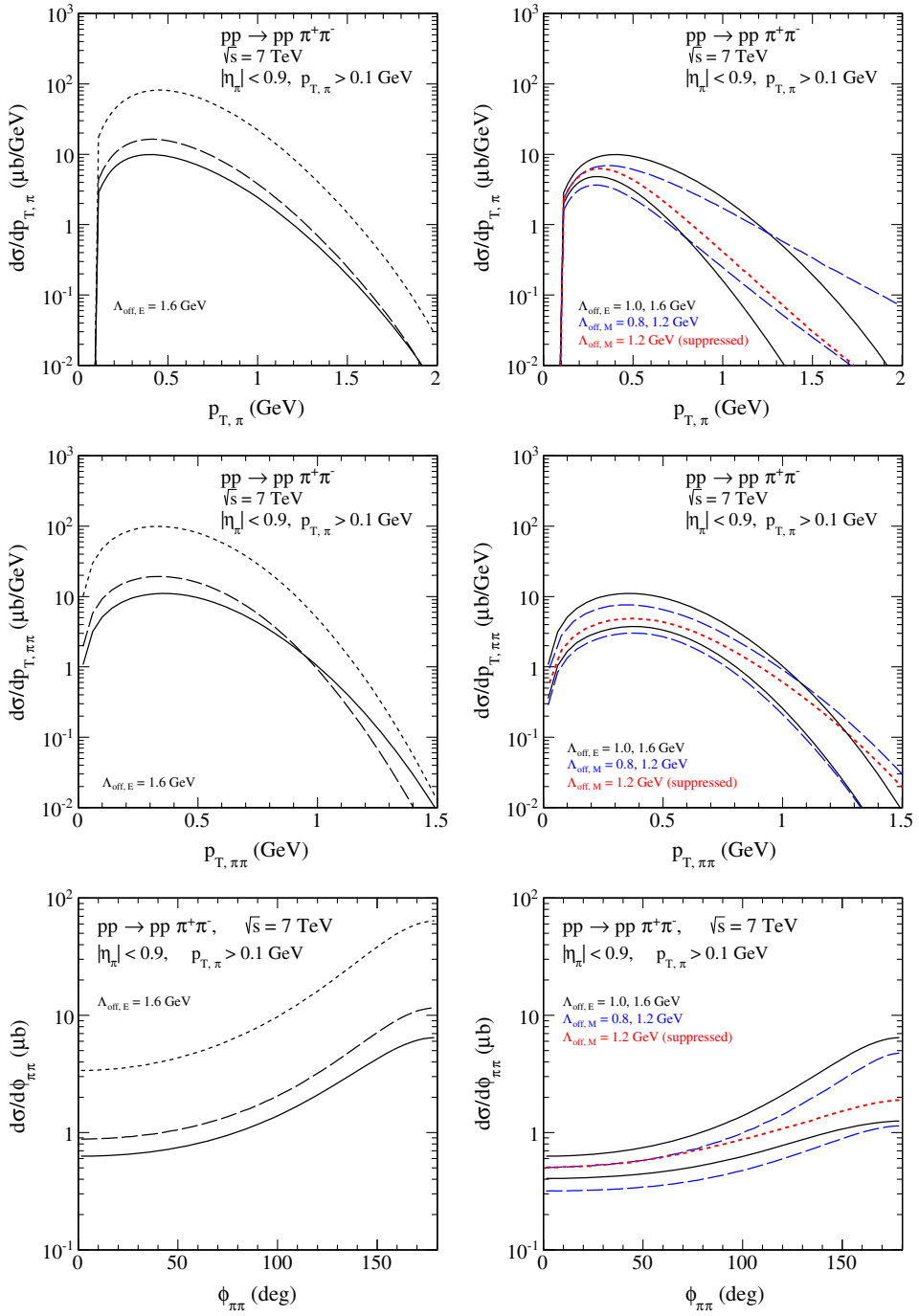

FIG. 11 (color online). Differential cross sections $d\sigma/dp_{t,\pi}$, $d\sigma/dp_{t,\pi\pi}$, and $d\sigma/d\phi_{\pi\pi}$ at $\sqrt{s} = 7$ TeV with the ALICE kinematical cuts specified in the legend. In the calculations we have used different values of the cutoff parameter $\Lambda_{\rm off}$.

$$\langle P_L(\cos\theta^{r.f.}_{\pi^+})\rangle(M_{\pi\pi}) = \frac{\int d\mathcal{PS} P_L(\cos\theta^{r.f.}_{\pi^+}) d\sigma/d\mathcal{PS}(M_{\pi\pi})}{\int d\mathcal{PS} d\sigma/d\mathcal{PS}(M_{\pi\pi})}, \tag{4.2}$$

where the integral is done over the experimental phase space. We have found, similar to the authors of [32], that the $\langle P_L(\cos\theta^{r.f.})\rangle(M_{\pi\pi})$ distributions are almost unaffected by the absorption effects; the thin and thick lines represent calculations without and with the absorption corrections. The difference between the results for form factors (2.12) and (2.13) is huge at higher invariant masses, and thus such observables may prove very useful in distinguishing between these choices. Preliminary

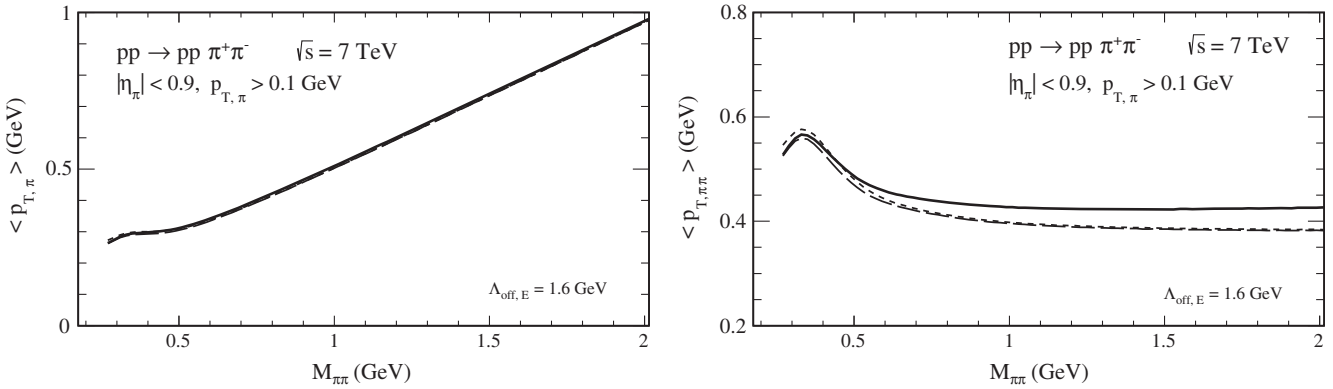

FIG. 12. Mean value of the $p_{t,\pi}$ (left panel) and $p_{t,\pi\pi}$ (right panel) as a function of two-pion invariant mass at $\sqrt{s} = 7$ TeV, with the ALICE kinematical cuts specified in the legend. In the calculation we have used the cutoff parameter $\Lambda_{\mathrm{off},E} = 1.6$ GeV.

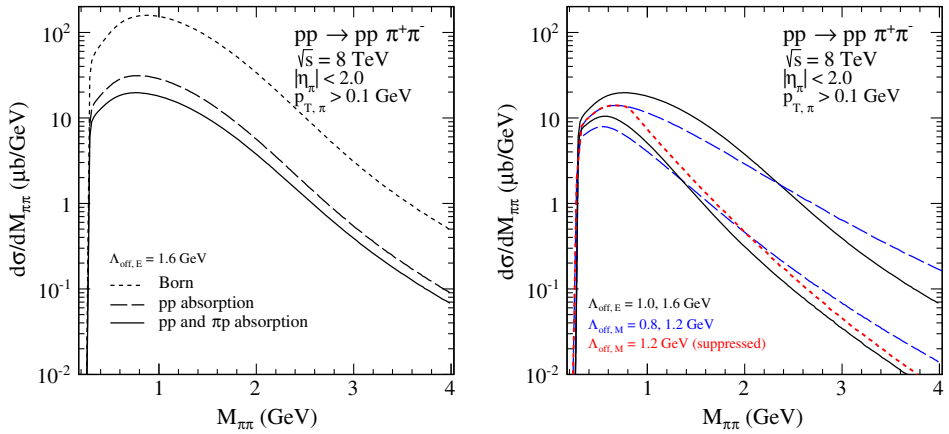

FIG. 13 (color online). Two-pion invariant mass distribution at $\sqrt{s} = 8$ TeV with the CMS kinematical cuts specified in the legend.

experimental results of the $\langle P_L(\cos\theta^{r.f.}_{\pi^+})\rangle(M_{\pi\pi})$ distributions for $\sqrt{s} = 1.96$ TeV are presented in Fig. 23 of [6] and strongly support our predictions calculated with the monopole form factors (2.13), particularly at higher two-pion invariant masses $M_{\pi\pi} > 1.5$ GeV; see also the discussion in Sec. 2.6.2 (Tevatron) of [27]. One can observe in Fig. 2.42 of [27] that the contribution of $L = 4$ is small at low $M_{\pi\pi}$ when the cuts are neglected (the left panels) and is significant already at $M_{\pi\pi} \approx 1$ GeV when the cuts are applied (the right panels). This suggests that the CDF kinematic cuts may distort the partial wave content. This makes conclusions more difficult.

C. ALICE experiment

Now, we shall present our predictions for experiments at the LHC. We shall start a review of our results for the case of the ALICE experiment at $\sqrt{s} = 7$ TeV. We impose the corresponding cuts on both pions' transverse momenta $p_{t,\pi} > 0.1$ GeV and pseudorapidities $|\eta_\pi| < 0.9$. In Fig. 10 we show two-pion invariant mass distribution. As for the case of the STAR experiment in the left panel, we show the Born result (the dotted line), the result with pp absorption only (the dashed line), as well as the results when including the extra πp absorption (the solid line). There is a similar tendency as in the STAR case. The extra absorption lowers the cross section without modifying the shape of the invariant mass distribution. In the right panel we show our result for two different forms of the off-shell form factor and different values of the cutoff parameters. As for the STAR case, the shape strongly depends on the form factor form as well as on values of the cutoff parameters.

Now we pass to distributions in transverse momenta of single pion and of the pion pair; see Fig. 11 (the top panels). The absorption effects due to πp interaction change the shape of the $p_{t,\pi\pi}$ distribution. Such a distribution can be easily measured by the ALICE Collaboration. The ALICE experiment cannot, however, register forward/backward protons. Therefore, only azimuthal correlations between pions can be measured. Our corresponding distribution is shown in Fig. 11 (the bottom panel). The $\phi_{\pi\pi}$ distribution

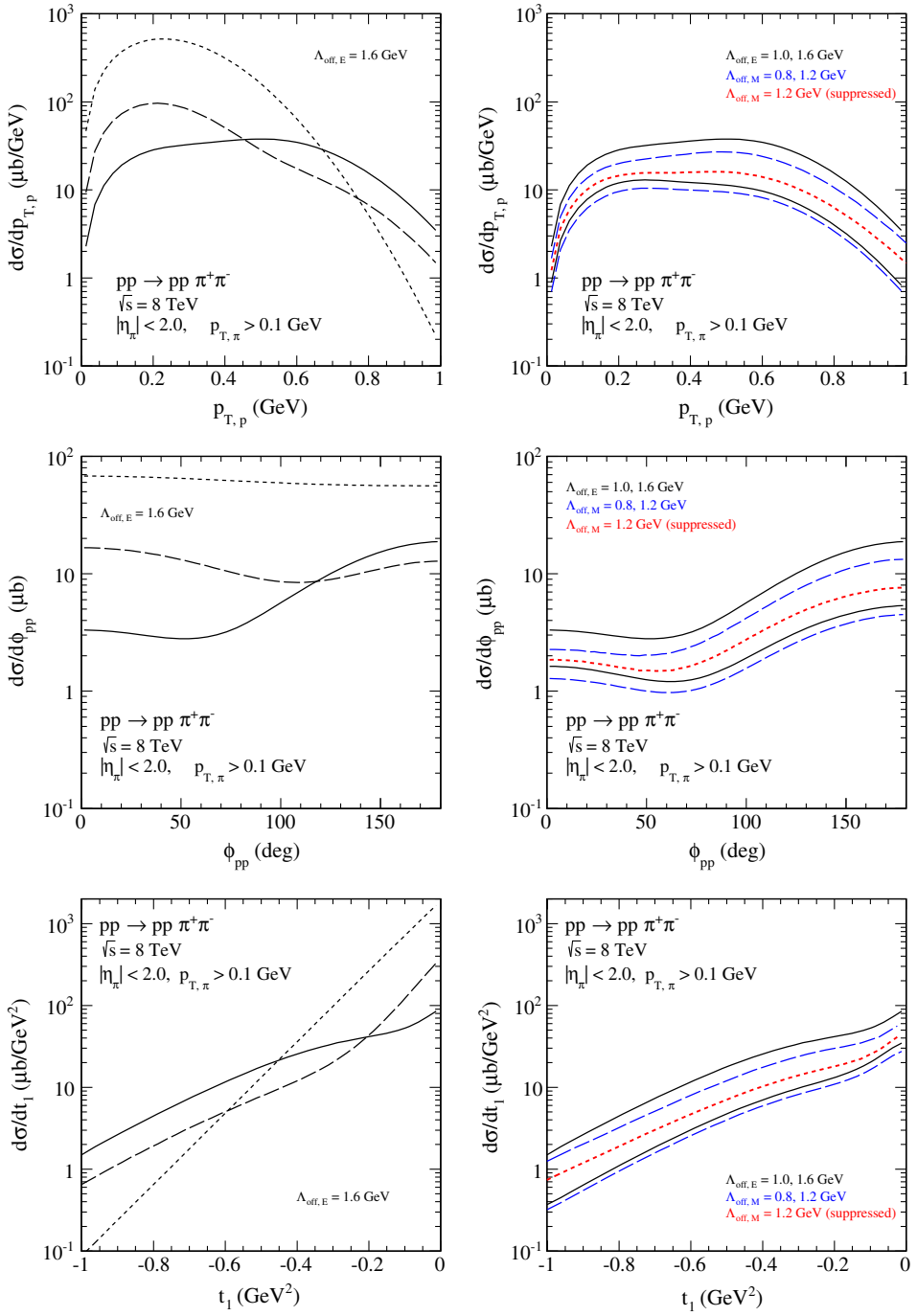

FIG. 14 (color online). The distributions in proton transverse momentum (top panels), in azimuthal angle between the outgoing protons (middle panels), and in proton four-momentum transfer t_1 (bottom panels) at $\sqrt{s} = 8$ TeV with the CMS kinematical cuts specified in the legend. In the left panels we show the distributions without and with the absorption corrections. In the calculation, results of which are shown on the right panels, we have used two forms for the off-shell pion form factors and different cutoff parameters $\Lambda_{\rm off}$.

peaks in the back-to-back configuration, i.e., when $\phi_{\pi\pi} = \pi$. The absorption effects practically do not change the shape of the distributions.

The average values of transverse momenta of single pion $\langle p_{t,\pi}\rangle(M_{\pi\pi})$ and of the pion pair $\langle p_{t,\pi\pi}\rangle(M_{\pi\pi})$ are shown in Fig. 12. The results have been obtained assuming that $p_{t,\pi} > 0.1$ GeV without the absorption effects (the dotted line), with the pp rescattering (the long-dashed line), and with the additional πp rescattering (the solid line).

D. CMS and ATLAS experiments

The ATLAS tracking detector provides a measurement of charged particle momenta in the $|\eta| < 2.5$ region. Since

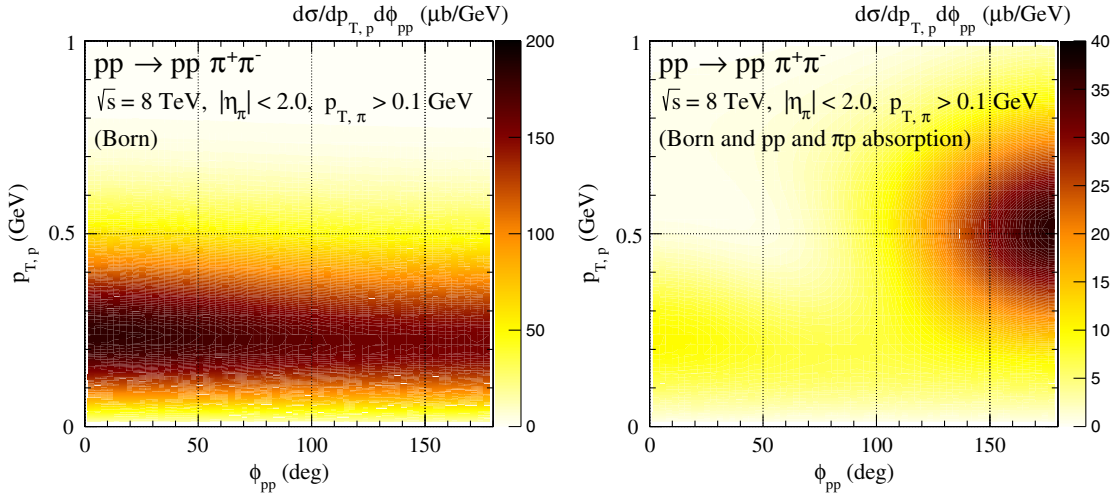

FIG. 15 (color online). Two-dimensional distributions in $p_{t,p}$ and ϕ_{pp} at $\sqrt{s} = 8$ TeV with the CMS kinematical cuts specified in the legend. We show the distributions without and with the absorption corrections. In this calculation we have used the cutoff parameter $\Lambda_{\mathrm{off},E} = 1.6$ GeV.

the correlation between the pseudorapidities of both pions is very large, the measurement can be performed independently using the tracking detector ($|\eta| < 2.5$) and the forward calorimeters ($2.5 < |\eta| < 4.9$); see Fig. 4 of [10]. We wish to note that the analysis in [10] was performed for $\Lambda^2_{\mathrm{off},E} = 2$ GeV^2 neglecting effect of the πN rescattering. Below, we shall show results of nonresonant model (including all rescattering corrections) for the CMS experiment and the corresponding kinematics cuts on both pions: $p_{t,\pi} > 0.1$ GeV and $|\eta_\pi| < 2.0$. The general features of the differential distributions for the ATLAS experiment are, however, similar.

In Fig. 13 we show two-pion invariant mass distribution. In the left panel we show again results for three cases: Born (the dashed line), absorption due to pp interaction (the long-dashed line), and the case with extra πp interaction (the solid line). In the right panel we show the dependence of the cross section on the choice of the pion off-shell form factor.

Both the CMS (when combined with TOTEM) and ATLAS (when combined with ALFA) collaborations can measure outgoing protons. What additional information can be provided by measuring the momenta of the outgoing protons? In Figs. 14 and 15 we show the influence of the absorption effects on the $p_{t,p}$, ϕ_{pp}, and t distributions. The distribution in proton transverse momenta are particularly interesting. The extra absorption effects due to πp interactions make the distributions much broader than in the case of the Born approximation, and even broader than in the case when only pp absorption effects are included. The effect depends on the value of cutoff parameter Λ_{off}. Therefore, we expect that the CMS and ATLAS experimental groups could verify our predictions. The extra absorption effects lead to

TABLE I. The integrated cross sections in μb for the central exclusive $\pi^+\pi^-$ production via the double Pomeron/$f_{2\mathbb{R}}$ exchange mechanism including the NN and πN absorption effects. The results for different experiments with cuts specified in Sec. IV and for the different values of the off-shell pion form factor parameters in Eqs. (2.12) and (2.13) are given.

$\sqrt{s}$ (TeV):	0.2	1.96	7	8	13
Cuts:	STAR (IV A)	CDF (IV B)	ALICE (IV C)	CMS (IV D)	CMS (IV D)
$\Lambda_{\mathrm{off},E} = 1.6$ GeV	0.23	3.69	6.57	23.92	28.64
$\Lambda_{\mathrm{off},E} = 1.0$ GeV	0.09	0.63	2.16	7.88	8.98
$\Lambda_{\mathrm{off},M} = 1.6$ GeV	0.26	6.45	9.12	33.60	40.92
$\Lambda_{\mathrm{off},M} = 1.2$ GeV	0.17 (0.13)[a]	2.48 (0.90)	4.65 (3.00)	17.14 (10.83)	20.65 (12.71)
$\Lambda_{\mathrm{off},M} = 0.8$ GeV	0.07	0.58	1.74	6.48	7.45

[a]The numbers in the parentheses show the resulting cross sections when multiplying by the suppression factor $f(M_{\pi\pi})$ given in section II.

a significant modification of the shape of proton-proton relative azimuthal angle distribution which also could be tested by the two experiments.[9] The distributions in proton four-momentum transfer $t = t_1 = t_2$ are presented in Fig. 14 (the bottom panels). The extra pion-proton interaction increases the distribution at large $|t|$.

The effect of absorption can be even better seen in two-dimensional distributions in proton-proton relative azimuthal angle and transverse momentum of one of the protons; see Fig. 15. Quite a different pattern can be seen for the Born case and for the case with full absorption. It is not clear to us whether such a two-dimensional distribution can be obtained in practice.

In Table I we have collected cross sections in μb for the exclusive $\pi^+\pi^-$ production with absorption effects discussed in Sec. III, and for some kinematical cuts specified in Sec. IV. The Born cross sections for $\sqrt{s} = 0.2$, 1.96, 7, and 8 TeV and $\Lambda_{\text{off},E} = 1.6$ GeV are 1.13, 39.60, 54.71, and 192.49 μb, respectively. Thus, the ratio of full and Born cross sections $\langle S^2 \rangle$ (the gap survival factor) is approximately 0.20 (STAR), 0.09 (CDF), or 0.12 (LHC). The large difference between $\sqrt{s} = 7$ TeV and $\sqrt{s} = 8$ TeV is first of all due to different cuts in different experiments (ALICE vs CMS). The results at $\sqrt{s} =$ 13 TeV were obtained also with the CMS kinematical cuts.

V. CONCLUSIONS

In the present paper we have taken into account absorption corrections due to pion-nucleon final state interaction in addition to those due to proton-proton interactions. To make realistic predictions of the cross sections the parameter responsible for off-shellness of intermediate pions in the Lebiedowicz-Szczurek model has been adjusted to experimental data. We have considered two different scenarios:

(1) The parameters have been adjusted to the STAR preliminary data [5], where protons have been registered, which guarantees exclusivity of the process. However, the statistics there was rather low and only low dipion invariant masses ($M_{\pi\pi} < 1.5$ GeV) could be observed.
(2) The parameters have been adjusted to the CDF data [7] (see also [6]), where only some rapidity gaps outside of the main detector were imposed in the experiment.

The cross section for the invariant masses $M_{\pi\pi} < 1$ GeV is subjected to low-energy pion-pion final state interaction ($\pi\pi$ FSI) effects which are not included in the present analysis. Thus, in the first scenario, one finds rather large $\Lambda_{\text{off}} \approx 1.6$ GeV in the region of $M_{\pi\pi} < 1$ GeV. In the second scenario, when the CDF data are fitted in the broad range of $M_{\pi\pi}$, one obtains $\Lambda_{\text{off}} \approx 0.8$ GeV. Then, as a consequence one underestimates the RHIC data at $M_{\pi\pi} \sim 0.5$–1.0 GeV. But this missing strength at low $M_{\pi\pi}$ is probably due to the low-energy $\pi\pi$ FSI enhancement in the σ meson region, see [25,47]. Therefore, we might expect that at higher masses the nonresonant model (with no Reggeization of intermediate pion) gives realistic predictions with the off-shell pion parameter $\Lambda_{\text{off}} \approx$ 1.0 GeV. The choice of monopole form for the pion off-shell form factors at large values of $M_{\pi\pi}$ is supported by the preliminary CDF results on the mean value of first even Legendre polynomials; see Fig. 9.

In our summary we wish to emphasize that it is probably impossible to describe within the present model (with the same parameters of the off-shell pion form factor) the CDF and STAR data. The reason is not completely clear at present. We do not feel competent to question the data. Instead, we wish to note that the kinematical range of both experiments is quite different. We expect that a possible explanation for the clear inconsistency is due to low-energy $\pi\pi$ final state interaction (enhancement of low $M_{\pi\pi}$ region, relevant for STAR and not so active for CDF) and interference of resonances and continuum (may depend on t_1 and t_2 that are very different for both experiments). These aspects should be addressed in the future.

We have proposed using a stretched exponential parametrization of πN amplitudes which better describes the large-t region and coincides with the exponential parametrization in small-t region. Such a parametrization is more adequate when focusing on larger transverse momenta. However, we have failed to describe the CDF data with $p_{t,\pi\pi} > 1$ GeV. Clearly, final tuning of the model requires to take into account both $\pi\pi$ FSI effects and explicit resonances such as the tensor $f_2(1270)$ meson. This goes beyond the scope of the present paper, where we have concentrated on the new absorption effects. This will be a subject of our future studies.

However, even the present, rather simplified treatment of the reaction mechanism allows us to draw interesting conclusions as far as the absorption effects are considered. The inclusion of the pion-nucleon interactions leads to additional damping of the cross section by a factor of about 2, almost independent of center-of-mass energy at least in the kinematic range considered in the present paper. The additional interaction changes the shape of some distributions ($d\sigma/dt_{1/2}$, $d\sigma/dp_{t,p}$, $d\sigma/d\phi_{pp}$), but leaves almost unchanged the shape of other distributions ($d\sigma/dM_{\pi\pi}$, $d\sigma/dy_\pi$, $d\sigma/dp_{t,\pi}$, $d\sigma/d\phi_{\pi\pi}$). Particularly spectacular modifications are obtained for $|t|$ and $p_{t,p}$ distributions. In particular, a measurement of the distribution in the relative azimuthal angle between the $\boldsymbol{p}_{t,1}$ and $\boldsymbol{p}_{t,2}$ vectors of the outgoing protons can provide a fully differential test of the soft survival factors. This could be

[9]Note that, in the case of the ATLAS experiment, the requirement of both protons being tagged in the ALFA detectors influences the shapes of the distributions only very little, but it reduces the cross section by a factor close to 3 [10].

verified in the future in experiments when both protons are measured, such as ATLAS/ALFA [10] or CMS/TOTEM [11]. In summary, the additional absorption effect discussed here seems crucial for a detailed understanding of the results of ongoing and planned experimental investigations.

ACKNOWLEDGMENTS

We are indebted to Mike Albrow, Lidia Görlich, Valery Khoze, Wolfgang Schäfer, Reiner Schicker, and Jacek Turnau for the interesting discussions. We are grateful to Maria Żurek for sending us the recent CDF data points. The work of P. L. was supported by NCN Grant No. DEC-2013/08/T/ST2/00165, MNiSW Grant No. IP2014 025173 "Iuventus Plus," and the START Fellowship from the Foundation for Polish Science. The work of A. S. was partially supported by NCN Grant No. DEC-2014/15/B/ST2/02528 (OPUS) and by the Centre for Innovation and Transfer of Natural Sciences and Engineering Knowledge in Rzeszów.

[1] M. G. Albrow, T. D. Coughlin, and J. R. Forshaw, Central exclusive particle production at high energy hadron colliders, Prog. Part. Nucl. Phys. **65**, 149 (2010).
[2] M. Albrow, Central exclusive production issue: Introduction, Int. J. Mod. Phys. A **29**, 1402006 (2014).
[3] A. Austregesilo *et al.* (COMPASS Collaboration), A partial-wave analysis of centrally produced two-pseudoscalar final states in pp reactions at COMPASS, *Proc. Sci.*, Bormio2013 (2013) 014.
[4] A. Austregesilo, Report No. CERN-THESIS-2014-190, 2014.
[5] L. Adamczyk, W. Guryn, and J. Turnau, Central exclusive production at RHIC, Int. J. Mod. Phys. A **29**, 1446010 (2014).
[6] M. Albrow, J. Lewis, M. Żurek, A. Święch, D. Lontkovskyi, I. Makarenko, and J. S. Wilson, Public note, Measurement of central exclusive hadron pair production in CDF, http://www-cdf.fnal.gov/physics/new/qcd/GXG_14/webpage/.
[7] T. A. Aaltonen *et al.* (CDF Collaboration), Measurement of central exclusive $\pi^+\pi^-$ production in $p\bar{p}$ collisions at $\sqrt{s} =$ 0.9 and 1.96 TeV at CDF, Phys. Rev. D **91**, 091101 (2015).
[8] R. Schicker *et al.* (ALICE Collaboration), in *Proceedings of Conference, EDS Blois Workshop, Qui Nhon, Vietnam, 2011*.
[9] R. Schicker, Diffractive production of mesons, EPJ Web Conf. **81**, 01005 (2014).
[10] R. Staszewski, P. Lebiedowicz, M. Trzebiński, J. Chwastowski, and A. Szczurek, Exclusive $\pi^+\pi^-$ production at the LHC with forward proton tagging, Acta Phys. Pol. B **42**, 1861 (2011).
[11] K. Österberg, Potential of central exclusive production studies in high β^* runs at the LHC with CMS-TOTEM, Int. J. Mod. Phys. A **29**, 1446019 (2014).
[12] A. Szczurek and P. Lebiedowicz, Exclusive scalar $f_0(1500)$ meson production for energy ranges available at the GSI Facility for Antiproton and Ion Research (GSI-FAIR) and at the Japan Proton Accelerator Research Complex (J-PARC), Nucl. Phys. **A826**, 101 (2009).
[13] W. Ochs, The status of glueballs, J. Phys. G **40**, 043001 (2013).
[14] A. Kirk, A review of central production experiments at the CERN Omega spectrometer, Int. J. Mod. Phys. A **29**, 1446001 (2014).
[15] C. Ewerz, M. Maniatis, and O. Nachtmann, A model for soft high-energy scattering: Tensor Pomeron and vector Odderon, Ann. Phys. (Amsterdam) **342**, 31 (2014).
[16] P. Lebiedowicz, O. Nachtmann, and A. Szczurek, Exclusive central diffractive production of scalar and pseudoscalar mesons; tensorial vs. vectorial Pomeron, Ann. Phys. (Amsterdam) **344**, 301 (2014).
[17] P. Lebiedowicz, O. Nachtmann, and A. Szczurek, ρ^0 and Drell-Söding contributions to central exclusive production of $\pi^+\pi^-$ pairs in proton-proton collisions at high energies, Phys. Rev. D **91**, 074023 (2015).
[18] P. Lebiedowicz, R. Pasechnik, and A. Szczurek, Measurement of exclusive production of scalar χ_{c0} meson in proton-(anti)proton collisions via $\chi_{c0} \to \pi^+\pi^-$ decay, Phys. Lett. B **701**, 434 (2011).
[19] L. A. Harland-Lang, V. A. Khoze, M. G. Ryskin, and W. J. Stirling, The phenomenology of central exclusive production at hadron colliders, Eur. Phys. J. C **72**, 2110 (2012).
[20] P. Lebiedowicz and A. Szczurek, Exclusive $pp \to nn\pi^+\pi^+$ reaction at LHC and RHIC, Phys. Rev. D **83**, 076002 (2011).
[21] A. Cisek, P. Lebiedowicz, W. Schäfer, and A. Szczurek, Exclusive production of ω meson in proton-proton collisions at high energies, Phys. Rev. D **83**, 114004 (2011).
[22] P. Lebiedowicz and A. Szczurek, Exclusive $pp \to pp\pi^0$ reaction at high energies, Phys. Rev. D **87**, 074037 (2013).
[23] P. Lebiedowicz and A. Szczurek, Exclusive $pp \to pp\pi^+\pi^-$ reaction: From the threshold to LHC, Phys. Rev. D **81**, 036003 (2010).
[24] Y. I. Azimov, V. A. Khoze, E. M. Levin, and M. G. Ryskin, Estimates of the cross-sections for double-Reggeon processes, Sov. J. Nucl. Phys. **21**, 215 (1975).
[25] J. Pumplin and F. S. Henyey, Double Pomeron exchange in the reaction $pp \to pp\pi^+\pi^-$, Nucl. Phys. **B117**, 377 (1976).
[26] B. R. Desai, B. C. Shen, and M. Jacob, Double Pomeron exchange in high-energy pp collisions, Nucl. Phys. **B142**, 258 (1978).
[27] P. Lebiedowicz, Ph.D. thesis, Institute of Nuclear Physics Polish Academy of Sciences, 2014, http://www.ifj.edu.pl/msd/rozprawy_dr/rozpr_Lebiedowicz.pdf.

[28] R. Waldi, K. R. Schubert, and K. Winter, Search for glueballs in a Pomeron Pomeron scattering experiment, Z. Phys. C **18**, 301 (1983).

[29] A. Breakstone *et al.* (ABCDHW Collaboration), Inclusive Pomeron-Pomeron interactions at the CERN ISR, Z. Phys. C **42**, 387 (1989).

[30] A. Breakstone *et al.* (ABCDHW Collaboration), The reaction Pomeron-Pomeron $\to \pi^+\pi^-$ and an unusual production mechanism for the $f_2(1270)$, Z. Phys. C **48**, 569 (1990).

[31] R. Kycia, J. Chwastowski, R. Staszewski, and J. Turnau, GenEx: A simple generator structure for exclusive processes in high energy collisions, arXiv:1411.6035.

[32] L. A. Harland-Lang, V. A. Khoze, and M. G. Ryskin, Modelling exclusive meson pair production at hadron colliders, Eur. Phys. J. C **74**, 2848 (2014).

[33] A. Donnachie, H. G. Dosch, P. V. Landshoff, and O. Nachtmann, *Pomeron Physics and QCD*, Cambridge Monographs on Particle Physics, Nuclear Physics and Cosmology Vol. 19 (Cambridge University Press, Cambridge, England, 2002), p. 1.

[34] C. W. Akerlof, R. Kotthaus, R. L. Loveless, D. I. Meyer, I. Ambats *et al.*, Hadron-proton elastic scattering at 50 GeV/c, 100 GeV/c and 200 GeV/c momentum, Phys. Rev. D **14**, 2864 (1976).

[35] D. S. Ayres *et al.* (Fermilab Single Arm Spectrometer Group), $\pi^\pm p$, $K^\pm p$, pp and $\bar{p}p$ elastic scattering from 50 GeV/c to 175 GeV/c, Phys. Rev. D **15**, 3105 (1977).

[36] Z. Asa'd *et al.* (Annecy (LAPP), CERN, Copenhagen (Niels Bohr Institute), Genoa, Oslo, and University College London Collaborations), Elastic scattering of charged mesons, antiprotons and protons on protons at incident momenta of 20, 30 and 50 GeV/c in the momentum transfer range $0.5 < -t < 8$ (GeV/c)^2, Nucl. Phys. **B255**, 273 (1985).

[37] A. Schiz, L. A. Fajardo, R. Majka, J. N. Marx, P. Nemethy *et al.*, A high statistics study of $\pi^+ p$, $\pi^- p$, and pp elastic scattering at 200 GeV/c, Phys. Rev. D **24**, 26 (1981).

[38] R. Rubinstein, W. Baker, D. P. Eartly, J. Klinger, A. J. Lennox *et al.*, Large-momentum-transfer elastic scattering of $\pi^\pm$, $K^\pm$, and $p^\pm$ on protons at 100 and 200 GeV/c, Phys. Rev. D **30**, 1413 (1984).

[39] A. Donnachie and P. V. Landshoff, pp and $\bar{p}p$ total cross sections and elastic scattering, Phys. Lett. B **727**, 500 (2013).

[40] M. G. Ryskin, A. D. Martin, and V. A. Khoze, High-energy strong interactions: From "hard" to "soft", Eur. Phys. J. C **71**, 1617 (2011).

[41] S. Fazio, R. Fiore, L. Jenkovszky, and A. Salii, Unifying "soft" and "hard" diffractive exclusive vector meson production and deeply virtual Compton scattering, Phys. Rev. D **90**, 016007 (2014).

[42] L. L. Jenkovszky, A. I. Lengyel, and D. I. Lontkovskyi, The Pomeron and Odderon in elastic, inelastic and total cross sections at the LHC, Int. J. Mod. Phys. A **26**, 4755 (2011).

[43] V. A. Khoze, A. D. Martin, and M. G. Ryskin, t dependence of the slope of the high energy elastic pp cross section, J. Phys. G **42**, 025003 (2015).

[44] A. Cisek, W. Schäfer, and A. Szczurek, Exclusive photoproduction of charmonia in $\gamma p \to Vp$ and $pp \to pVp$ reactions within k_t-factorization approach, J. High Energy Phys. 04 (2015) 159.

[45] J. Orear, Transverse Momentum Distribution of Protons in p-p Elastic Scattering, Phys. Rev. Lett. **12**, 112 (1964).

[46] P. Lebiedowicz, R. Pasechnik, and A. Szczurek, Exclusive production of $\chi_c(0^+)$ meson and its measurement in the $\pi^+\pi^-$ channel, Nucl. Phys. B, Proc. Suppl. **219–220**, 284 (2011).

[47] K. L. Au, D. Morgan, and M. R. Pennington, Meson dynamics beyond the quark model: A study of final state interactions, Phys. Rev. D **35**, 1633 (1987).

[48] L. A. Harland-Lang, V. A. Khoze, M. G. Ryskin, and W. J. Stirling, Central exclusive meson pair production in the perturbative regime at hadron colliders, Eur. Phys. J. C **71**, 1714 (2011).